Submitted June 2007

Detection and Classification of Weld Discontinuities in Radiographic Images (Part I: Supervised Learning)

by Germano X. de Pádua,* Romeu R. da Silva,† Domingo Mery,‡ Marcio H.S. Siqueira,§ João M.A. Rebello** and Luiz P. Calôba††

ABSTRACT

Radiographic testing of weld joints is of great importance for verifying and maintaining weld quality. This work presents a new technique for the development of an automatic or semiautomatic system for radiographic weld analysis. This technique uses gray level profiles transversal to weld beads in radiographic patterns. These profiles were processed to aid in the setup of nonlinear pattern classifiers developed by neural networks with algorithms by backpropagation of error. The classification accuracy was estimated via the average correctness of 10 randomly chosen test sets. The results presented a general accuracy of classification correctness of around 95% for the class patterns in the profiles that were used.

Keywords: *transversal gray level profiles, nonlinear classifier, weld discontinuities, radiography, nondestructive testing.*

INTRODUCTION

Nondestructive testing is increasingly used as a tool to evaluate equipment and material quality. Among the various test methods, radiographic testing is often favored because of its ability to create an image of the internal structure of the item under test (Halmshaw, 1994). However, technical reports are subjective because they are based on visual analysis of radiographs, and depend on the experience of the examiner and the test adjustment parameters, even with a radiographic image of satisfactory quality (Fücsök et al., 2000; Fücsök et al., 2002).

The technological advances of digital radiographic imaging equipment, coupled with recent developments in artificial intelligence (such as artificial neural networks, fuzzy logic, neuro-fuzzy systems and genetic algorithms), have provided the impetus for active work on the development of automatic and semiautomatic systems for analyzing and classifying radiographic images.

Radiographic testing is widely used for welded joints, and a large amount of research has gone into the acquisition of images and development of software to interpret weld bead radiographs. This work presents the classification results for weld discontinuities imaged in radiographs taken by international institutions.

* Petróleo Brasileiro SA – Petrobras, 81 Alm. Barroso Av., 27th floor, Rio de Janeiro, Brazil; e-mail <germanox@petrobras.com.br>.

† Pontificia Universidad Católica de Chile, Departamento de Ciencia de la Computación, Av. Vicuna Mackenna 4860 (143), Santiago, Chile.

‡ Pontificia Universidad Católica de Chile, Departamento de Ciencia de la Computación, Av. Vicuna Mackenna 4860 (143), Santiago, Chile; e-mail <dmery@ing.puc.cl>.

§ Rua General Canabarro, 500-9° andar, Ala D, CEP: 20271-900, Rio de Janeiro, Brazil.

** Department of Metallurgical and Materials Engineering, Federal University of Rio de Janeiro (UFRJ), PO Box 68505, CEP 21945-970, Rio de Janeiro, Brazil.

†† Department of Electrical Engineering, Federal University of Rio de Janeiro (UFRJ), PO Box 68504, CEP 21945-970, Rio de Janeiro, Brazil.

The main objective of the work is to evaluate the performance of nonlinear pattern classifiers, set up by artificial neural networks, in the detection and classification of the main classes of weld discontinuities (undercutting, lack of penetration, lack of fusion, porosity, slag inclusion and cracking). A new methodology was used, which will be described in detail in this paper. This methodology is based on the extraction of transversal gray level profiles of the weld beads to be used as input data in the classifiers, a resource that other authors have used, but with different classification techniques (Liao and Li, 1998; Liao and Ni, 1996; Liao et al., 1999). These profiles were preprocessed using a procedure distinct from that used in other works, in order to optimize the classification of the discontinuities. The accuracy of the classification was estimated through the use of randomly chosen training and test sets, and the generalization of the classifiers was assured by using validation sets. The results are presented in classifier performance tables and compared with the results of other work.

This work is a continuation of works already published (Padua et al., 2003; Padua et al., 2004), and is the first part of the obtained results in this study using transversal line profiles as an input set of neural networks. The second part is about using unsupervised learning developed by adaptive resonance theory with some modifications (Haykin, 1994).

STATE OF THE ART

There are a number of excellent works in this area that could be discussed here. However, taking into consideration the objective of this work, the most relevant are the publications of Liao and Ni (1996) and Liao and Li (1998). These works also made use of transversal profiles of weld beads, but with methodologies different from those developed in the present work.

Liao and Ni (1996) extracted the weld bead from the radiographic digital image using the software Khoros. However, neural networks weren't used for the classification of the beads. In this work, Liao and Ni described in detail the 15 steps that make up the algorithm of bead extraction. Their results proved the total efficiency of his methodology (100% success rate) for the extraction of weld beads that had linear edges/borders. They emphasized, however, the need to develop this technique for weld beads with curved edges/borders.

In later work, Liao and Li (1998) described their efforts to develop an automatic radiographic system for the detection of discontinuities in the weld bead. The methodology employed was developed based on observations that an intensity profile of the gray levels transversal to the weld bead took the shape of a perfect bell. A welding discontinuity, if apparent in the weld bead, resulted in an anomaly in the shape of the profile. Liao and Li classified these anomalies into three categories: peak, trough and slant-concave.

The detection technique used by Liao and Li (1998) was made up of four main steps:

- a preprocessing module
- a curve adjustment module
- an anomaly profile detection module
- a postprocessing module.

The preprocessing module was used to remove the background of the image and place all the images on the same gray standard. The curve adjustment module was used to soften the profiles by applying a filter. The anomaly profile detection module detected the existence of anomalies in the profiles. The results obtained from the processed profiles were then assembled to generate a bi-dimensional map of the discontinuity. The postprocessing module removed isolated anomalies that had been identified in a previous step.

MATERIALS AND METHODOLOGIES

Radiographic Films and Scanners

To give the greatest possible reliability to the results of the classification, radiographic images from the International Institute of Welding (IIW) and the Federal Institute of Materials Research and Testing (BAM) were used. The largest possible number of radiographs was used in order to obtain the best possible statistical significance from the results. An older collection of radiographic images from the IIW was digitized with a scanner using a spatial resolution of 20 pixels per millimeter and 256 levels of gray. The second collection of radiographs from the IIW was recently digitized using a scanner with the maximum available resolution of 79 pixels per millimeter. The collection of radiographs from BAM was digitized using a scanner with 24 pixels per millimeter and 12 bits of gray level, later converted to 8 bits (256 levels). Although these images showed various types of weld discontinuities, only the more common classes of welding discontinuities, such as undercutting, lack of penetration, lack of fusion, porosity, slag inclusion and longitudinal cracking, were studied. In addition, the "no discontinuity" class was also studied. Figure 1 shows examples of the radiographic images used for each class of discontinuity (Silva et al., 2005).

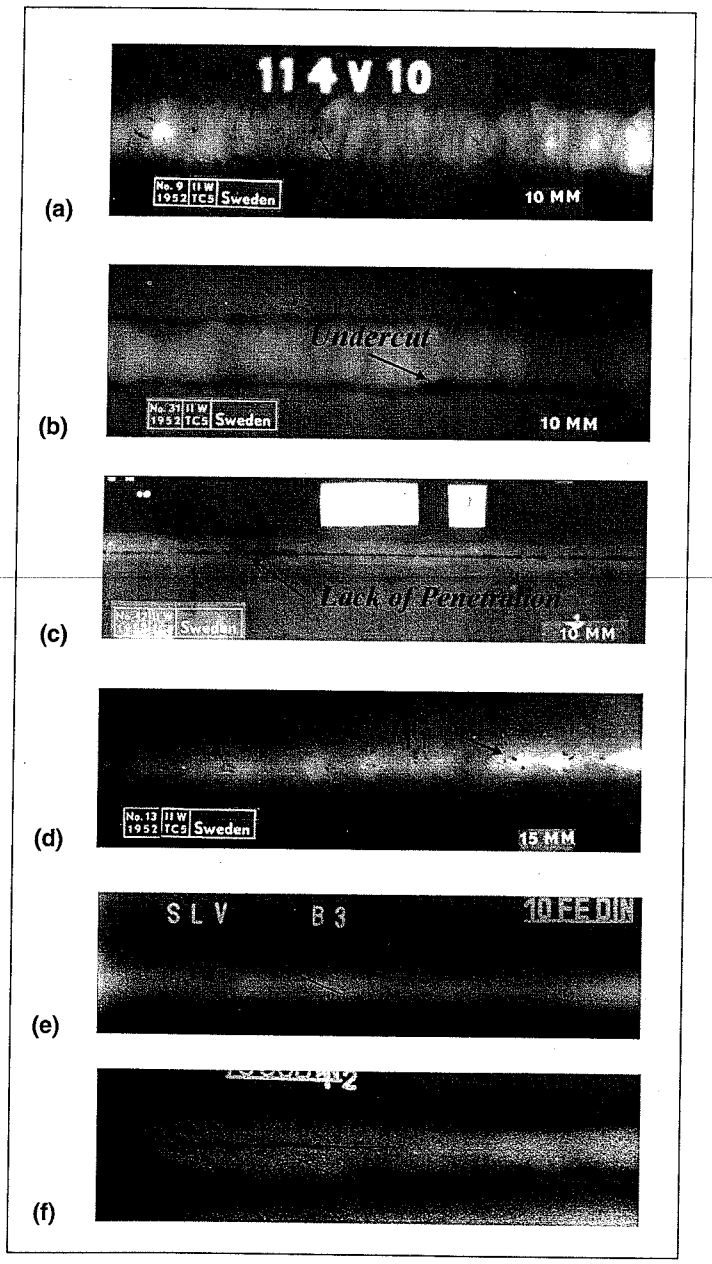

Figure 1 — Examples of radiographic images used for each class of discontinuity (Silva et al., 2005): (a) slag inclusion; (b) undercutting; (c) lack of penetration; (d) porosity; (e) lack of fusion; (f) cracking.

Data Preprocessing

The digitalized radiographs were preprocessed with a 3×3 filter to reduce noise (Silva et al., 2001; Silva et al., 2002; Gonzalez and Woods, 1992) and to enhance contrast mainly of the weld bead and for subsequent procedures.

Most work in this research area involves processing complex images for segmentation of the weld joint image, extraction of the features of the "objects" detected in the segment, and discontinuity classification (Shafeek et al., 2004a; Shafeek et al., 2004b; Silva et al., 2001; Silva et al., 2004; Wang and Liao, 2002). A final solution applicable to the various types of radiographs has yet to be found, however. In this work, a procedure using transversal gray level profiles of the beads was employed, not only in the presence of joint discontinuities, but in the discontinuity class as well. The technique used in this work is innovative and more practical from the point of view of developing semiautomatic or automatic systems for the detection and classification of weld discontinuities in radiographs.

Figure 2 illustrates didactically the shape of the transversal gray level profile of a weld bead in a radiograph. The vertical axis corresponds to a scale of gray (normally 256 levels), while the horizontal axis corresponds to the vertical dimension of the weld. Since the aim of the work is only to find and classify discontinuities present in the weld, the horizontal parameter of the graph, which represents the base metal region, can be discarded to reduce computational calculations and optimize the development of the classifiers.

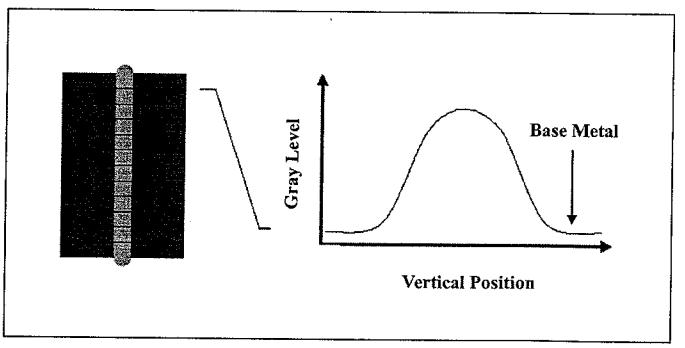

Figure 2 — Example of a transversal gray level profile of a weld bead in a radiograph (in this case, without discontinuities).

The part of the image corresponding to the weld bead was visually extracted from the whole image so that the profiles traced contained the least amount of irrelevant information possible for the development of the classifier. It is enough to point out that the follow-up to this work will involve the development of an image processing technique for the automatic extraction of the bead, which will later be connected to classifier algorithms developed in this work. Figure 3 illustrates the extraction of the bead image from the rest of the radiograph. Before the extraction of the weld bead, the images were calibrated spatially as shown in Figure 3 so that the transversal profiles had a precise vertical bead measurement.

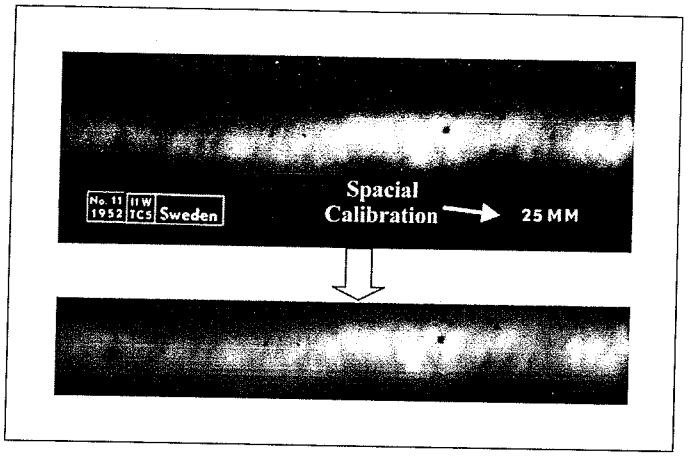

Figure 3 — An example of a radiographic image used, showing identification label and calibration measurement, and the respective bead image extracted from the original pattern.

The profiles were extracted from each weld image using a software program with a simple transversal line technique (visual detection of the discontinuity). The number of profiles available for each discontinuity class was as such:

- lack of fusion: 64
- undercutting: 95
- lack of penetration: 151
- slag inclusion: 154
- cracking: 265
- porosity: 412
- no discontinuities: 467.

After acquisition of the profiles (signals), three types of processing were carried out.

- First, the profiles were standardized in relation to their respective amplitudes; a procedure carried out by dividing each point of the profile by its maximum gray level value so that all the profiles had amplitudes situated on the scale from zero to one.
- Second, the profiles were treated for noise reduction by using the low-pass Savitzky-Golay filter, which has the advantage of not altering the amplitudes of the signals as much as the average mobile filter. Empirically, the best performance of this filter was obtained for an operational window with eight points and polynomial of the second order. Taking into account that the original radiographic images had different resolutions, due to their distinct origins and the equipment available at the time of film digitization, the profiles contained a quantity of distinct points making the correct implementation of the classifiers impossible. In this case, the profiles were interpolated using the fast Fourier transform technique so that they would contain the same number of profile points with the smallest size (276).
- Third, the discontinuities are situated randomly in the vertical dimension of the bead, except lack of penetration, which is normally found in the center of the profile. This variation of position certainly increases the intraclass variation, making the training of the classifiers more difficult and therefore affecting their performance. Consequently, it was deemed that all the discontinuities should be adjusted to a position to the right of the average (center) of an estimated gauss curve based on each profile (Liao and Li, 1998; Liao and Ni, 1996; Liao et al., 1999). The profiles that originally contained discontinuities situated to the right of the peak or in the center of the gauss curve did not need to have their position inverted.

Figure 4a shows an example of an original profile with standardization of amplitude and number of points, but without noise reduction. Figure 4b shows the same profile after application of the low-pass filter. Figure 4c shows the profile after inversion of the discontinuity position in relation to the center of the adjusted gauss curve.

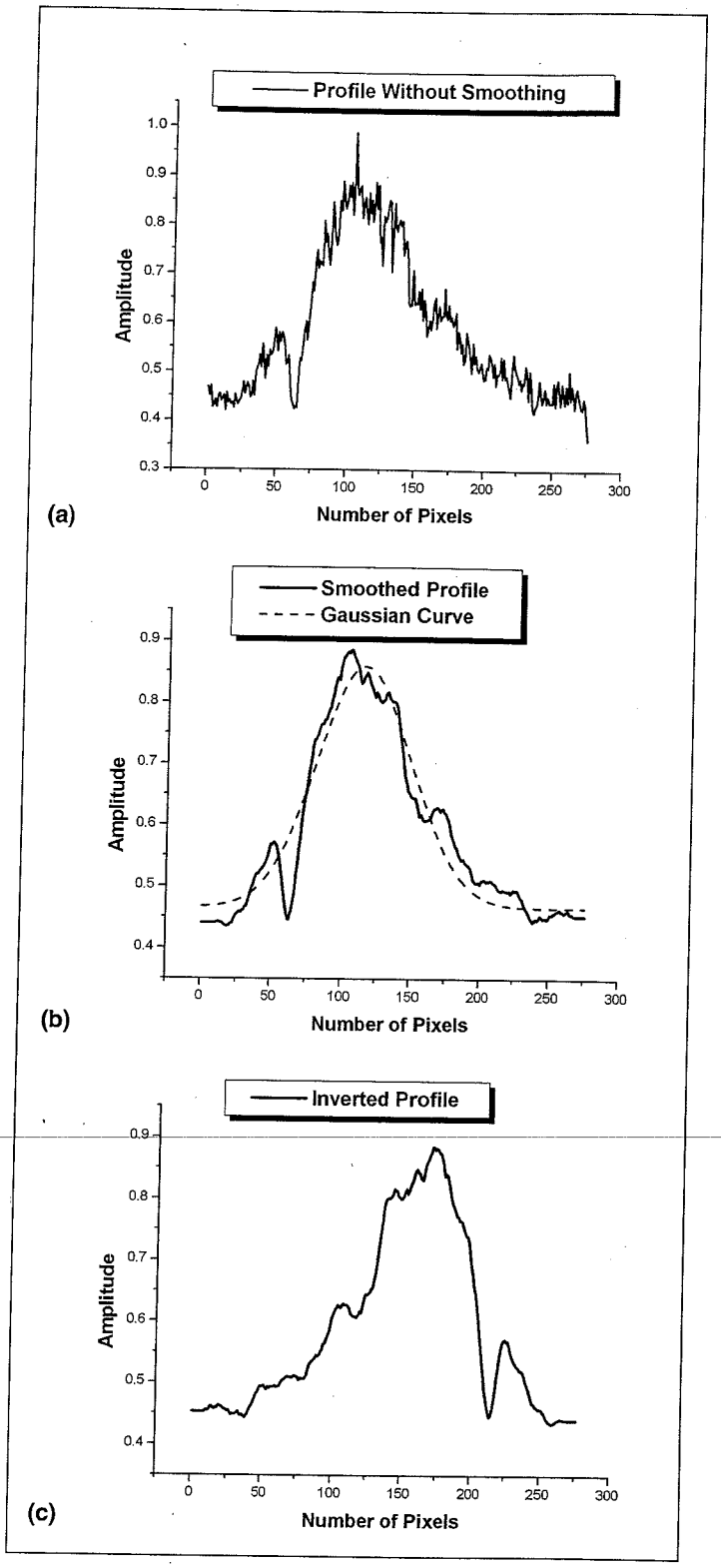

Figure 4 — Profile filtering and adjustment: (a) original profile with standardization of amplitude and number of points; (b) profile after application of Savitzky-Golay filter and the gauss curve; (c) profile after inversion of discontinuity position in relation to the center of the gauss curve.

Nonlinear Pattern Classifiers: Architecture and Classifier Training

The nonlinear classifiers were implemented with neural networks of two trained layers with algorithms for backpropagation of error (Haykin, 1994). The output layers of the networks contained seven neurons of the hyperbolic tangent type due to the seven

Table 1 Optimization of the number of neurons in the intermediate layer of the nonlinear classifier

Number of Neurons in the Intermediate Layer	Training Set Data		Test Set Data	
	With Reclassification	Without Reclassification	With Reclassification	Without Reclassification
10	100	99.93	97.72	96.89
20*	100	100	99.38	97.72
30	100	100	98.96	97.10
40	100	100	98.14	95.45

* best result with the test data

classes of patterns present in the data. A question that occurs in the development of a nonlinear classifier regards knowing the ideal number of neurons that should be used to permit the best performance of the classifier. In this work, the number of neurons used in the intermediate layers was varied and the performance obtained for a pair of randomly chosen sets for training and testing were observed. The training was carried out up to 3000 epochs or error of training equal to 0.001, using a learning ratio α variable and moment $\beta = 0.9$ (Haykin, 1994), adjustments that allowed for faster convergence of training after empirical tests.

Nonlinear Pattern Classifiers: Accuracy of the Classifiers

One of the greatest concerns in recognizing the patterns is the estimated accuracy of the classifiers that can be calculated using weighted averages of correctness between the training and test data (Diamantidis et al., 2000; Efron and Tibshirani, 1993; Efron and Tibshirani, 1995; Silva et al., 2005).

The pronounced difference in the quantity of data between the pattern classes studied could favor the correctness classification of those classes with more data in terms of developing a training algorithm for backpropagation of error. A large amount of data tends to significantly influence the calculation of training error. In this case, an acceptable solution that, in the majority of cases, produces good results, is replicating data of the class with the least number of data until it reaches the number of data of the most favored class. In order, then, to estimate the classification accuracy of the nonlinear classifier used in this work, ten random selections of pairs for training and testing sets were carried out in the following manner: 15% were extracted from the total of the discontinuity-free class, which had the largest quantity of data (467), to make up the test sets (this percentage was chosen empirically). That is to say, 69 data were chosen for test sets and the others were left over to make up the training sets (398 data). The same was done with the other classes once their data had been replicated until they reached the number of data for training and testing sets as in the discontinuity-free class. All classes then had 69 data for test sets and 398 data for training sets. This procedure guaranteed that the chosen data for testing sets were not used for training sets, and all classes had the same quantity of data for the two sets.

The classifier performance results, as well as the estimated accuracy (here considered the arithmetic mean of the performances obtained with the test sets), are presented in the tables. Also, the confusion tables of classification between classes are presented for the set with the performance nearest to the estimated accuracy.

RESULTS AND DISCUSSIONS

Optimization of the Number of Neurons in the Intermediate Layer

After carrying out the random selections as described above, a study was carried out to optimize the number of neurons to be used in the intermediate layer of the nonlinear classifier with these new sets, using only a pair of training/testing sets among the ten selected. In order to control overtraining and guarantee generalization of the classifier, 15% of the training data were extracted (85% of the original data) to make a validation set. Table 1 shows the results obtained, where it is evident that only 20 neurons in the intermediate layer obtained 100% of correctness with the training data and 97.72% for the test data under the most conservative conditions (without reclassification) and 99.38% of correctness with reclassification, the best indices of correctness with the testing set. The classification criterion for reclassification considers the greatest output neuron (in this case, seven outputs due to seven pattern classes) of the classifier as the indicator of the tested pattern class input. The without reclassification criterion is the most conservative because it uses as the output class indicator the only positive output. These criteria of classification are explained in detail by Silva et al. (2001).

Figure 5 shows the training and test curves resulting from training with the 20 neurons in the intermediary layer, showing that the training was interrupted with fewer than 1000 epochs due to validation control.

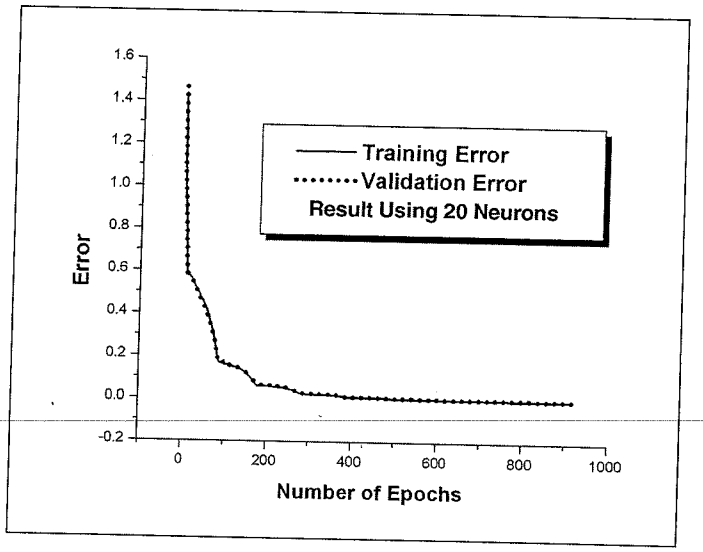

Figure 5 — Training error and validation error curves using 20 neurons in the intermediate layer.

Estimated Accuracy of Classification

Table 2 contains all the results of the performance obtained with the test sets chosen for the with and without reclassification criteria, as well as the number of epochs of interruption of training by the validation control. The criteria of validation was fixed in 100 epochs, that is, if the error of validation was maintained unaltered or grew over 100 epochs, training was interrupted and the values of the synapses and bias (Haykin, 1994) were adjusted to the values that resulted in the smallest error of validation.

The resultant average correctness, for our estimate of classification accuracy, was 95.0% for the test data without reclassification, a very satisfactory index. With reclassification, it reached 98.4% correctness, an index very close to that obtained on average with the training sets (about 100%). Another result worth mentioning is the small standard deviation –2.1% for the test data without reclassification. This proves the reliability of the classification accuracy estimation and the classification of the main types of welding discontinuities present in traversal gray level profiles submitted to preprocessing. The generalization of the classifier was proven in the

Table 2 Calculation of the classification accuracy for the nonlinear classifier

Data Sets	Training Data		Test Data		Number of Epochs
	With Reclassification	Without Reclassification	With Reclassification	Without Reclassifiation	
1	100	100	100	99.0	920
2	100	100	98.6	93.4	1044
3	100	100	98.0	94.6	948
4	100	100	97.6	92.0	923
5	100	100	98.0	94.6	940
6*	100	100	97.3	95.3	940
7	100	100	99.0	96.7	939
8	100	100	97.8	92.1	1044
9	100	100	99.4	97.1	949
10	100	100	98.2	95.5	1135
Mean	100	100	98.4	95.0	
Mean σ	0	0	0.9	2.1	

* set that was closest to the average
σ = standard deviation

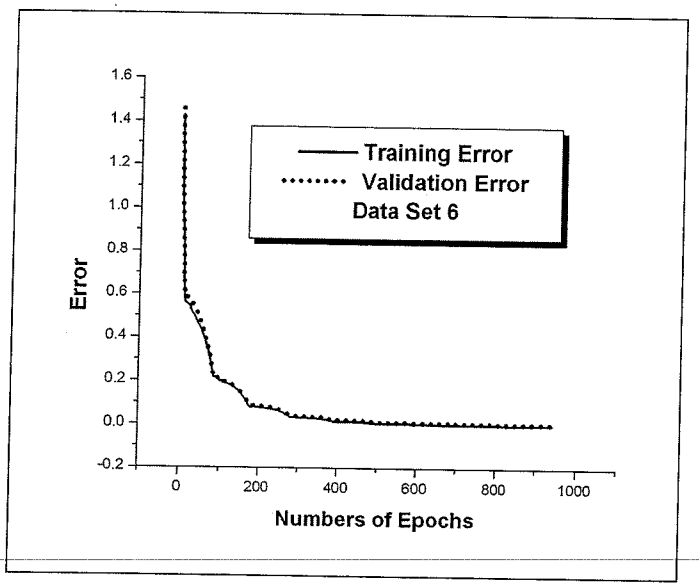

Figure 6 — Training and validation error curves using 20 neurons in the intermediate layer of set six.

small differences in performance between the training and testing sets. Figure 6 shows the training and validation curves of the sixth set of Table 2, the set that was closest to the average (the one that could be considered the most representative in terms of correctness of classification expected).

In Table 2 there is only the general average correctness of all classes, as well as the indices of each set, without an idea of the correctness and errors of each class. Thus, Table 3 was set up, referring to the sixth set of Table 2 that represents the indices of correctness and error (confusion) of each class with respect to the other classes. In this type of table, we have the lack of fusion class in the first line and in the first column of Table 3. This class's result was 53 correctly classified data among the 69 used in the test set. Sixteen profiles were classified with *no* class, that is to say, all the outputs of the neurons were negative, remembering that in the condition of Table 3 one class only is indicated when it has only one positive output among the seven neurons of the seven classes studied. For the lack of penetration class, 66 data were correctly classified and three data confused with the porosity class, and so on for the other classes. Note that in Table 3, all the profiles were classified correctly for the undercut and sag inclusion classes. Table 4 gives the same information, but with indices of correctness and confusion in percentages. It is worth noting once again that Tables 3 and 4 are for the most conservative situation of classification with the test data. For the case of

Table 3 Confusion table for test set 6 for the results without reclassification (results of confusion in quantity of profiles)

	Lack of Fusion	Lack of Penetration	Undercut	Crack	Slag Inclusion	Porosity	No Discontinuity	None	More than One
Lack of fusion	53	0	0	0	0	0	0	16	0
Lack of penetration	0	66	0	0	0	3	0	0	0
Undercut	0	0	69	0	0	0	0	0	0
Crack	0	0	2	67	0	0	0	0	0
Slag inclusion	0	0	0	0	69	0	0	0	0
Porosity	0	0	0	0	0	68	0	1	0
No discontinuity	0	0	0	0	0	0	68	1	0

Table 4 Confusion table for test set 6 for the results without reclassification (results of confusion in percentage of correctness/error)

	Lack of Fusion	Lack of Penetration	Undercut	Crack	Slag Inclusion	Porosity	No Discontinuity	None	More than One
Lack of fusion	76.81%	0	0	0	0	0	0	23.19%	0
Lack of penetration	0	95.65%	0	0	0	4.35%	0	0	0
Undercut	0	0	100%	0	0	0	0	0	0
Crack	0	0	2.9%	97.1%	0	0	0	0	0
Slag inclusion	0	0	0	0	100%	0	0	0	0
Porosity	0	0	0	0	0	98.55%	0	1.45%	0
No discontinuity	0	0	0	0	0	0	98.55%	1.45%	0

Table 5 Confusion table for test set 6 for the results with reclassification (results of confusion in quantity of profiles)

	Lack of Fusion	Lack of Penetration	Undercut	Crack	Slag Inclusion	Porosity	No Discontinuity
Lack of fusion	61	0	0	8	0	0	0
Lack of penetration	0	66	0	0	0	3	0
Undercut	0	0	69	0	0	0	0
Crack	0	0	2	67	0	0	0
Slag inclusion	0	0	0	0	69	0	0
Porosity	0	0	0	0	0	69	0
No discontinuity	0	0	0	0	0	0	69

Table 6 Confusion table for test set 6 for the results with reclassification (results of confusion in percentage of correctness/error)

	Lack of Fusion	Lack of Penetration	Undercut	Crack	Slag Inclusion	Porosity	No Discontinuity
Lack of fusion	88.41%	0	0	11.59%	0	0	0
Lack of penetration	0	95.65%	0	0	0	4.35%	0
Undercut	0	0	100%	0	0	0	0
Crack	0	0	2.9%	97.1%	0	0	0
Slag inclusion	0	0	0	0	100%	0	0
Porosity	0	0	0	0	0	100%	0

reclassification, error indices are even less, as can be seen in Table 5 in terms of quantity of data and Table 6 in percentage terms.

Table 6 shows that the no discontinuity, porosity and sag inclusion classes present indices of 100% correctness for set 6, and only for the lack of penetration and crack classes have small indices of confusion with the porosity and undercut classes, respectively. The largest index of confusion was the lack of fusion class with the crack class (11.59%), which is not critical, since both discontinuities imply a rejection and repair of the weld according to norms and international codes.

In general terms of classification, the results are extremely satisfactory since the estimated accuracy even for the most conservative situation was 95.0%, a value above the results obtained in other works (Liao and Ni, 1996; Silva et al., 2004). It is evident that these results were possible due to the processes carried out on the profiles before being used in the development of the classifiers, something that had not been done in previous works (Padua et al., 2003; 2004). It should also be pointed out that the results obtained in this work have greater reliability from the statistical point of view due to the amount of data used, as well as the number of sets used to estimate the classification accuracy. The use of gray level profiles is more promising for the development of automatic radiographic testing systems for weld joints, since it does not require the complicated techniques of image segmentation and extraction of the discontinuity characteristics to create the input data for the classifiers. These complicated techniques make it more difficult to develop a system that can be applied efficiently on various types of radiographic joint images existing in the industrial field. This work can already be considered a detection algorithm for operational discontinuities, since the "no discontinuity" class was not confused with any other type of discontinuity.

The work presented here will be continued with research directed toward the development of the first part of the system, extraction of weld beads from the radiographs and automatic acquisition of transversal profiles. This latter part will afterwards be connected to the algorithms developed for the work presented here. Some work has already been done on this by Felisberto et al. (2006).

CONCLUSION

Using the classification results presented here, it is shown that the transversal profiles can be used as input data in the nonlinear classifiers for identification and classification of the main types of discontinuities, giving good classification results. The profiles must first be put through a Savitzky-Golay filter for noise reduction, undergo standardization of amplitude and quantity of points, and have the position of the discontinuities adjusted, reducing interclass variance. The optimization of the number of neurons used in the intermediate layer, as well as the utilization of validation sets to control the best moment to interrupt training, permitted the generalization of the classifier for the test sets. The methodology applied is capable of distinguishing signals with and without discontinuities without creating classification errors.

The techniques presented in this work are innovative, and are an incentive to continue to work for the development of an automatic or semiautomatic system for interpretation of digitized radiographs of soldered equipment.

ACKNOWLEDGMENTS

The authors wish to acknowledge the National Council for Scientific and Technological Development, CAPES (Higher Level Training Agency), FAPERJ (Research Foundation from Rio de Janeiro) and ANP (Brazilian Agency for Petroleum) for financial support and scholarships. They also acknowledge the International Institute of Welding and the Federal Institute of Materials Research and Testing of Berlin for permission to publish the radiographic images used in the present work. This work has been partially supported by a grant from the School of Engineering at Pontificia Universidad Católica de Chile.

REFERENCES

Diamantidis, N.A., D. Karlis and E.A. Giakoumakis, "Unsupervised Stratification of Cross-Validation for Accuracy Estimation," *Artificial Intelligence*, Vol. 116, 2000, pp. 1–16.

Efron, B. and R.J. Tibshirani, *An Introduction to the Bootstrap*, New York, Chapman and Hall/CRC, 1993.

Efron, B. and R.J. Tibshirani, *Cross-Validation and the Bootstrap: Estimating the Error Rate of the Prediction Rule. Technical Report 477*, Stanford University, 1995. Available at: <http://utstat.toronto.edu/tibs/research.html>.

Felisberto, M.K., H.S. Lopes, T.M. Centeno and L.V.R. Arruda, "An Object Detection and Recognition System for Weld Bead Extraction from Digital Radiographs," *Computer Vision and Image Understanding*, Vol. 102, No. 3, 2006, pp. 238–249.

Fücsök, F., C. Müller and M. Scharmack, "Reliability of Routine Radiographic Film Evaluation – An Extended ROC Study of the Human Factor," *Eighth European Conference on Nondestructive Testing*, Barcelona, EFNDT, 2002, p. 439.

Fücsök, F., C. Müller and M. Scharmack, "Human Factors: The NDE Reliability of Routine Radiographic Film Evaluation," *15th World Conference on Nondestructive Testing*, Rome, ICNDT, 2000, p. 758.

Gonzalez, R.C. and R.E. Woods, *Digital Image Processing*, Reading, Massachusetts, Addison-Wesley, 1992.

Halmshaw, R., *Industrial Radiography*, Mortsel, Belgium, Agfa-Gevaert NV, 1994.

Haykin, S., *Neural Networks – A Comprehensive Foundation*, Upper Saddle River, New Jersey, Macmillian, 1994.

Liao, T.W. and Y. Li, "An Automated Radiographic NDT System for Weld Inspection: Part II – Flaw Detection," *NDT&E International*, Vol. 3, No. 3, 1998, pp. 183–192.

Liao, T.W., D. Li and Y. Li, "Detection of Welding Flaws from Radiographic Images with Fuzzy Clustering Methods," *Fuzzy Sets and Systems*, Vol. 108, 1999, pp. 145–158.

Liao, T.W. and J. Ni, "An Automated Radiographic NDT System for Weld Inspection: Part I – Weld Extraction," *NDT&E International*, Vol. 29, No. 3, 1996, pp. 157–162.

Padua, G.X., R.R. Silva, J.M.A. Rebello and L.P. Calôba, "Extração do Cordão-de-Solda e Detecção de Defeitos em Radiografias Usando Redes Neurais," *Third Panamerican Conference for Nondestructive Testing (PANNDT)*, 2003, pp. 1–8.

Padua, G.X., R.R. Silva, J.M.A. Rebello and L.P. Calôba, "Classification of Welding Defects in Radiographs Using Transversal Profiles to the Weld Seam," *16th World Conference on Nondestructive Testing*, Montreal, WCNDT, 2004, pp. 90–91.

Shafeek, H.I., E.S. Gadelmawla, A.A. Abdel-Shafy and I.M. Elewa, "Automatic Inspection of Gas Pipeline Welding Defects Using an Expert System," *NDT&E International*, Vol. 37, No. 4, 2004a, pp. 301–307.

Shafeek, H.I., E.S. Gadelmawla., A.A. Abdel-Shafy and I.M. Elewa, "Assessment of Welding Defects for Gas Pipeline Radiographs Using Computer Vision," *NDT&E International*, Vol. 37, No. 4, 2004b, pp. 291–299.

Silva, R.R., M.H.S. Siqueira, L.P. Calôba and J.M.A. Rebello, "Radiographic Pattern Recognition of Welding Defects Using Linear Classifiers," *Insight*, Vol. 43, 2001, pp. 669–674.

Silva, R.R., M.H.S. Siqueira, L.P. Calôba and J.M.A. Rebello. "Evaluation of the Relevant Feature Parameters of Welding Defects and Probability of Correct Classification Using Linear Classifiers," *Insight*, Vol. 44, 2002, pp. 616–622.

Silva, R.R., M.H.S. Siqueira, L.P. Calôba and J.M.A. Rebello, "Pattern Recognition of Weld Defects Detected by Radiographic Test," *NDT&E International*, Vol. 37, 2004, pp. 461–470.

Silva, R.R., M.H.S. Siqueira, L.P. Calôba and J.M.A. Rebello, "Estimated Accuracy of Classification of Defects Detected in Welded Joints by Radiographic Tests," *NDT&E International*, Vol. 38, 2005, pp. 335–348.

Wang, G. and T.W. Liao, "Automatic Identification of Different Types of Welding Defects in Radiographic Images," *NDT&E International*, Vol. 35, 2002, pp. 519–528.